EXPERIMENT INVESTIGATION ON HIGH-SPEED GRINDING OF K9 OPTICAL GLASS

Bei ZHANG[1]

K9 glass is a kind of high performance optical material that is widely used in aeronautics and astronautics. However, the requirement of ground surface roughness is very strict and the grinding cost is very high. In order to solve the problem and take modern grinding theory into account, the high-speed grinding is greatly improved to solve the K9 grinding problem. Experiment research on high-speed grinding of K9 glass is carried out by using monolayer brazed diamond grinding wheel in the paper. The surface topography of grinding wheel and ground surface before and after dressing are observed. The surface roughness, the surface roughness ratio Rz/Ra and the ratio of normal and parallel Ra direction are measured. The results show that with the increase of grinding speed, the surface defects and surface roughness are reduced; the continuity of surface texture is improved, and the cutting process tends to be ductile. According to theoretical analysis, it shows that the grinding surface roughness changes with the grinding process parameters, and the performance of K9 glass material is inversely proportional to the grinding energy.

Keywords: High-speed grinding, K9 glass, brazed diamond grinding wheel, surface roughness

1. Introduction

K9 glass is an excellent optical material that is widely used in aeronautics and astronautics field. However, K9 glass is a kind of material that is brittle and difficult to cut. Generally, surface and subsurface defect easily appear in the process of glass materials [1]. Many experiment researches have put forward their solutions. SH.Yin developed a high-precision slicing machine. It is found that the fastening mode, cutting blade and cutting water flow have influence on the chipping size and surface roughness of glass slices [2]. J. Du proposed a model of influencing factors to control the edge chipping of glass drilling, which involves material stress, additional supports, feed rate in addition to diamond grit size and concentration [3]. HN.Li believed that subsurface defect can be avoided when the surface roughness of optical glass Rz is

[1] Henan University of Science & Technology, Luoyang, Henan, 471003, China, E-mail: zhangbei_607@126.com

less than 1.5μm [4]. QL. Zhang investigated the surface generation mechanism on WC/Co and reaction bonded Si/SiC by high-speed grinding and quasi static indentation test. It is discovered that different removal features appear for different compound material in high-speed grinding. With the increase of cutting depth, the cemented carbide has ductile zone, grain spalling and grain breakage, while SiC/Si has ductile zone, phase boundary fracture and crushing [5]. J. Cheng develops a newmicro drill-grinding tool for precision microdrilling of soda-lime glass and proposed a micro drill-grinding force model [6]. A resin coat on workpiece surface is constructed to change the mechanical condition of local ground surface material and the experiment is carried out. The result indicates that fracture size decreases from 239 μm to 15 μm and the feed rate increases from 50nm/rev to 200nm/rev without decreasing the ductile regime.

K9 glass is a kind of brittle material and obeys the same law of brittle material grinding. Based on Miyashita and Bifano theory, when the machining size reaches the microscopic field, the plastic deformation in metal cutting is more likely to occur in micro-grinding. ST. Chen designed a micro machine tool with intelligent feedback unit, which can provide grinding depth of several nanometers [7]. The result indicates that the ductile regime machining of quartz glass is realized. The surface roughness can reach Ra0.056 μm when the cutting depth is 1μm and the grinding velocity is 50-70m/min. B. Guo[8] presents a micro-structuring strategy of grain surface in coarse-grained diamond grinding wheel by laser machining. It is known that when the diamond grain of large grit size is cut into micro-groove by laser dressing, the surface roughness and subsurface damage depth can be decreased remarkably. QL. Zhao used the three precision conditioned coarse-grained diamond wheels with different grain sizes [9]. In the surface grinding of BK7, all three precision conditioned coarse-grained diamond wheels can produce high surface quality in terms of a low sub-surface damage depth less than 3 μm and a much small surface roughness value around Ra 1nm.

High-speed grinding can reduce wheel wear, improve surface quality and reduce grinding force. It is a promising way to solve the problem of ceramic or glass processing. K. Zhan investigated the cylindrical and internal high-speed grinding of silicon nitride ceramic spindle [10]. The result indicated that the ground surface roughness tends to decrease linearly with the grinding velocity. J. Kaionchaiyakul [11] has done a lot of experiments on testing of hot pressed silicon nitride and aluminum nitride. It is discovered that high-speed grinding can reduce ceramic damage without reducing the material removal rate. In low speed grinding, there will be discrete scratches due to brittle regime. In high-speed grinding surface, the texture becomes continuous and smooth, and the plastic flow is evident.

High-speed grinding of K9 optical glass is another solution, which can reduce the requirement of grinding and dressing equipment. High-speed grinding is relatively easy, which is directly oriented to the engineering application of K9 optical glass. However, there are few reports on high-speed grinding of K9 optical glass until now.In the paper, high-speed grinding is used to improve the surface quality of K9 optical glass, and the grinding performance of K9 optical glass is analyzed.

2. Material and Research Method

The grinding experiment is carried out on BLOHM MT408 grinding machine. High temperature brazing technology is used for brazing diamond grinding wheel. The substrate of grinding wheel is Φ260×127×18mm, the diamond is YK-7 and the grit size is 150μm. The grain is evenly distributed, the grain spacing is 1mm and the plunge grinding is adopted. The grinding fluid is 5% water-based emulsion. The size of K9 glass workpiece is 30×12×8mm. The workpiece performance is shown in Table 1.

Table 1

K9 glass material performance

Material performance	value
Density/g/cm^3	2.5
Young modulus/GPa	81
Vicker hardness/GPa	6.9
Fracture toughness/MPa.m$^{1/2}$	0.8

Firstly, the grinding wheel is installed on the spindle, and the flange of the tune wheel is adjusted to ensure that the radial runout is less than 10μm. And then the cup dressing is used. The dressing parameter is shown in Table 2 and the dressing equipment is removed before grinding. The grinding process parameters are shown in Table 3.

Table 2

Dressing Process Parameters

Process parameter	value
Wheel revolution rate/r/mi	300n
Cup wheel revolution rate/r/min	9000
Dressing depth of cut/μm/pass	5
Cumulative dressing allowance/μm	30
coolant	5%water-based emulsion

Table 3

Grinding process parameters

Process parameter	value
grinding velocity/m/s	20,40,70,100
Depth of cut/μm	5
Workpiece speed/mm/min	30,300,3000
method	plunge
Grinding fluid	5%water-based emulsion

3. Results

3.1 grinding wheel surface topography

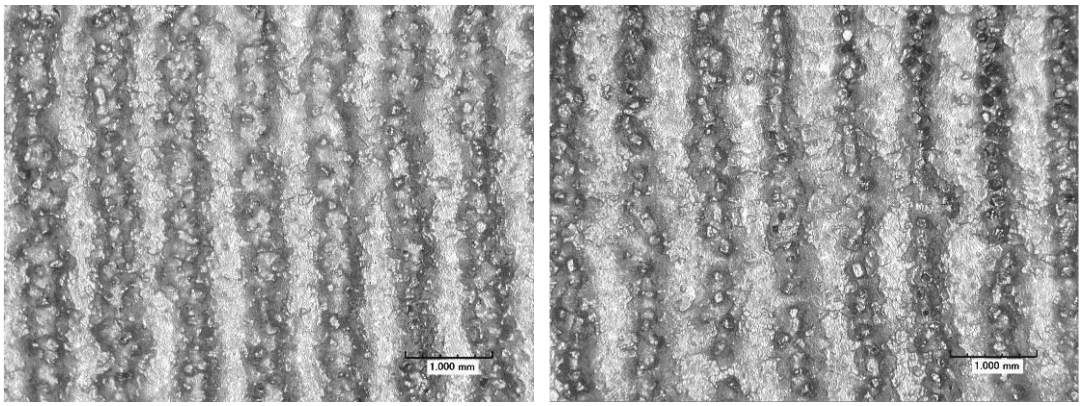

(a) before dressing (b) after dressing

Fig.1 The surface topography of monlayer brazed diamond grinding wheel before and after dressing

Fig 1 shows the surface topography before and after dressing. From Fig 1(a), it can be seen that before dressing, the grain has poor exposure and most grain is covered by brazing filler. From Fig 1(b), it can be seen that most grain has crystal shape, and the cover filler is removed. However, some filler also appear near the grain root.

3.2 K9 glass surface topography

Fig 2 shows the surface topography of ground K9 optical glass. Fig 2(a) is the ground surface with a cutting depth of 5μm, a workpiece of 30mm/min and a grinding velocity of 20m/s. Fig 2(b) is the ground surface with a cutting depth 5μm, a workpiece of 30mm/min and a grinding velocity of 100m/s. Fig 2 shows that the parallel texture is evident.

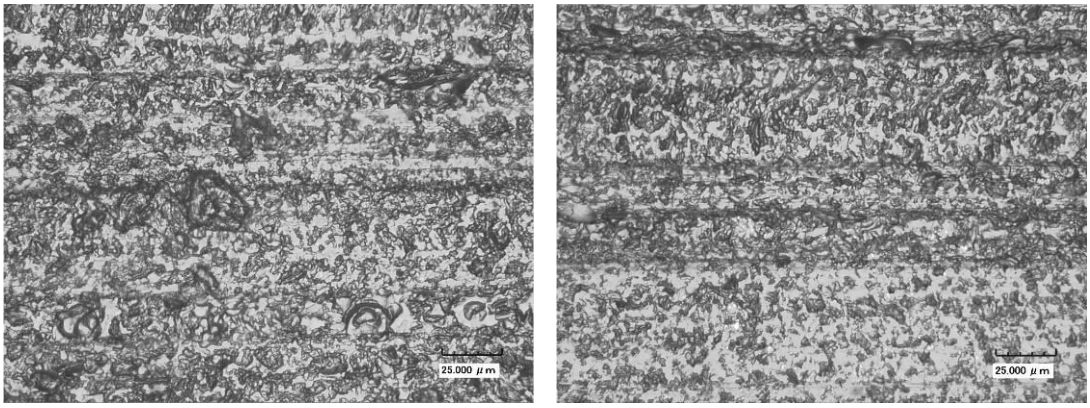

(a) v_s=20m/s (b) v_s=100m/s

Fig. 2. Ground surface topography of K9 glass (ap=5μm, vw=30mm/min)

From Fig 2(a), large defect with size of 25μm appear on the ground surface, which are distributed in the micro-grooves, while Fig 2(b) has few major defects. Generally, the removal mode is brittle, and the large pits are made by grain severe interference. Consequently, high-speed grinding induces thinner undeformed chip thickness and improves the removal mode.

3.3 K9 glass surface roughness

It is shown in Fig.3 that the surface roughness *Ra* of K9 glass varied with the process parameter between1.23-1.85μm. From Fig.3, it can be seen that *Ra* decreases with the increase of grinding velocity and increase with the increase of workpiece speed. Formula 1 shows that the undeformed chip thickness will decrease with the increase of grinding velocity and the decrease of workpiece speed. In other word, the undeformed chip thickness become close to the critical chip thickness, at which the removal mode will change from brittleness to ductileness. Then the removal mode becomes more ductile as shown in Fig.4. Due to the brittleness of the removal method, the fracture size becomes smaller, the chip thickness becomes thinner, the surface damage decreases and the continuity of wear marks increases. Consequently, the surface roughness is improved [12, 13].

$$h_m = \left[\frac{3}{C \tan\theta} \left(\frac{v_w}{v_s} \right) \left(\frac{a_p}{d_s} \right)^{1/2} \right]^{1/2} \tag{1}$$

Where, h_m is the undeformed chip thickness; the grain density C=2.5mm^{-2}; the grain half vertex angle θ=60^o; v_w is the workpiece speed; v_s is the grinding velocity; a_p is the cutting depth and d_s is the wheel diameter.

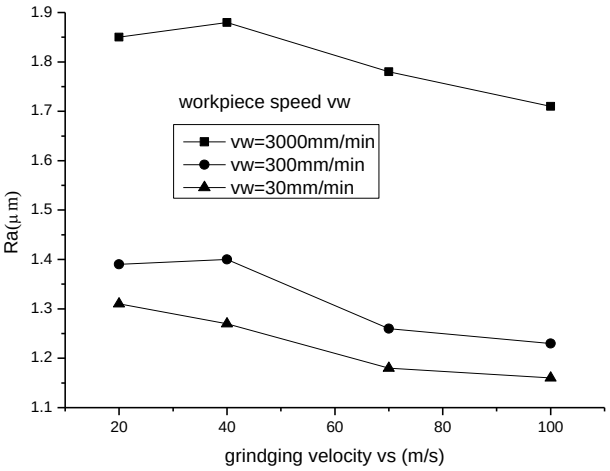

Fig. 3. Variation of Ra with grinding process parameter

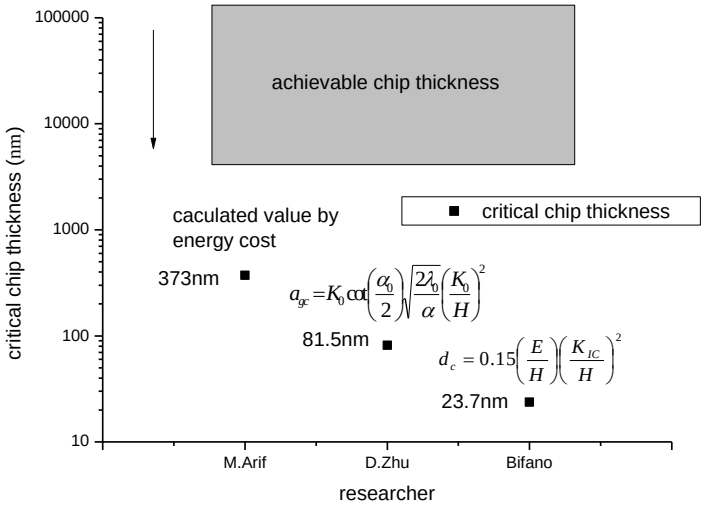

Fig. 4. The undeformed chip thickness and the critical grain cutting depth of K9

The variation of $\frac{Rz}{Ra}$ with grinding process parameters is shown in Fig 5. It is seen that $\frac{Rz}{Ra}$ varies from 5.13 to 6.70, which is in the described range 4-7 [14]. The

variation of $\frac{Rz}{Ra}$ with the workpiece speed is not remarkable. According to formula (2), it is known that *Rz* is proportional to h_i (grain interference), and h_i is proportional to the undeformed chip thickness h_m. From formula (1), it can be seen that when the grinding velocity increases, the chip thickness decreases, the grain interference decreases, and then *Rz* decreases. *Ra* shows the surface average unevenness, while *Rz* is the larger surface defect. Therefore, $\frac{Rz}{Ra}$ shows the role of larger defects in unevenness contribution. $\frac{Rz}{Ra}$ decreases with the increase of grinding velocity, which proves that high-speed grinding is benefit to reduce larger defects and improve surface uniformity [15].

$$\begin{cases} Rz = k_0 h_i - h_i / \sin\theta_i \\ h_i \propto h_m \end{cases} \tag{2}$$

Where, *Rz* is the micro height of ten point unevenness; k_0 is the coefficient that relative to K9 glass material and grain shape; h_i is the grain interference; θ_i is the angle between grain normal and horizontal plane and h_m is the undeformed chip thickness.

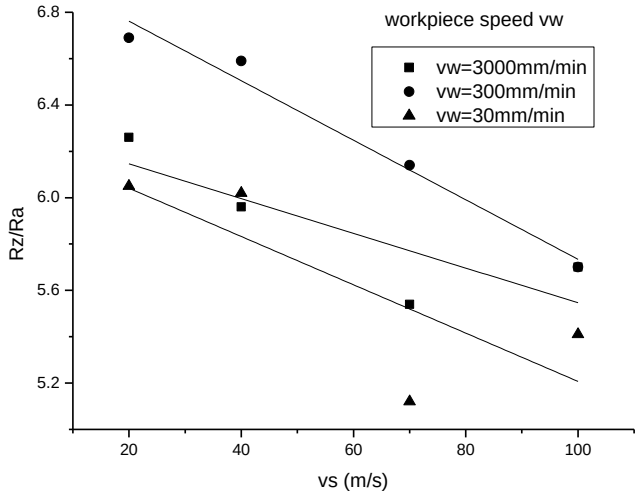

Fig. 5. Variation of $\frac{Rz}{Ra}$ with grinding process parameter

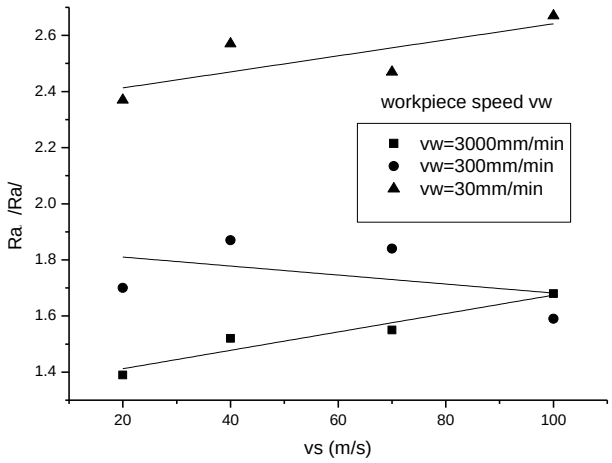

Fig. 6. Roughness ratio between normal and parallel direction $\frac{Ra\perp}{Ra//}$

Fig. 6 shows the ratio of *Ra* in the normal and parallel direction of grinding velocity. It can be seen that $\frac{Ra\perp}{Ra//}$ increases with the increase of grinding velocity and decreases with the increase of workpiece speed. Consequently, the analysis shows that K9 glass grinding is in brittle mode. The surface consists of fractured and spalled pits, which prevents the formation of continuous texture. The larger the pits are, the less the grooves are, and the worse the continuity of the grinding marks is. With the increase of grinding velocity and decrease of workpiece speed, pits become less and the continuity of grinding texture increase. Compared with the parallel direction, the unevenness along the normal direction of grinding velocity increases, thus $\frac{Ra\perp}{Ra//}$ increases.

4. Discussion

In order to reveal the influence of grinding process parameter on the surface roughness, a model is presented in formula (3) (4). From Fig 7, it can be seen that model 1 is close to the experiment data when the grinding velocity is low, and is quite different from the experiment data when grinding velocity is high. However, model 2 is very close to the experiment data. It follows that *Ra* is the power function of v_s. Model1 data is obtained by the profile maximum height in the surface, which has

obvious physical meaning. While the coefficient a and b in model 2 have no clear physical meaning. To sum up, it can be seen from the two models that the surface roughness can be predicted by grinding process parameters such as grinding speed and workpiece speed.

$$\text{Model 1: } Ra = \frac{1.36}{m} L^{6/5} \left(\cot\theta\right)^{2/5} \left(\frac{v_w}{v_s} \sqrt{\frac{1}{d_s}} \right)^{2/5} \tag{3}$$

Where, scale factor *m=4-7* ; grain spacing L=1mm; grain half vertex angle θ=60^0-75^0; v_w is the workpiece speed; v_s is the grinding velocity and the grinding wheel diameter d_s=260mm.

$$\text{Model 2: } Ra = a_1 \left(\frac{v_w}{v_s \left(\rho d_s\right)^{\frac{1}{2}}} \right)^{\frac{1}{2}} + b_1 \tag{4}$$

Where, a_1 and b_1 is the coefficient; v_w is the workpiece speed; v_s is the grinding velocity; grain edge radius ρ=0.03mm and grinding wheel diameter d_s=260mm.

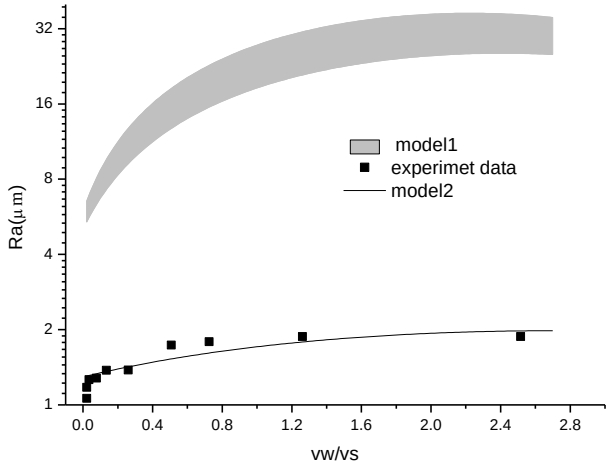

Fig. .7 Prediction model of surface roughness

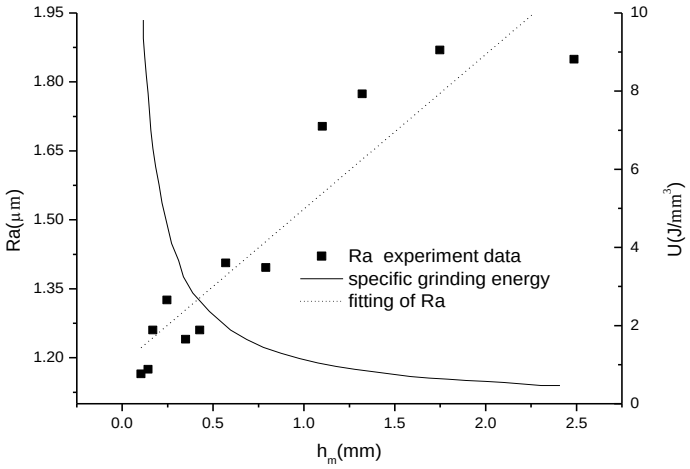

Fig. 8. Variation of specific grinding energy and surface roughness with chip thickness

The surface roughness of K9 glass is greatly influenced by the grinding process parameter. The brittle fracture size depends on the distance between the undeformed chip thickness and the critical chip thickness, which influence the surface uniformity. Consequently, the surface roughness must be relative to the magnitude of chip thickness. Fig. 8 shows the variation of ground surface roughness with chip thickness. From formula (1) and Fig.8, it can be seen that Ra is proportional to h_m. While h_m is proportional to the half power of v_w and inversely proportional to the half power of v_s. The relation between Ra and v_w, v_s is shown in formula (5).

$$Ra \propto \left(\frac{v_w}{v_s} \right)^{\frac{1}{2}} \tag{5}$$

Where: v_w is the workpiece speed and v_s is the grinding velocity.

According to TW, Hwang[16] and formula (6), the specific grinding energy of K9 glass is calculated. It can be seen that the relation between specific grinding energy and process parameter is shown in formula (7). Then the concise formula (8) is derived from formula (5) and (7), which indicates the inverse relation between the surface roughness and specific grinding energy. Formula not only describes the correlation between surface roughness and grinding process parameter, but also describes the correlation of ground material performance (referenced by k_0 in formula (2)). Based on the fitting data of Fig.8 and the calculated value of specific grinding

energy, the smooth curve of K9 glass is shown in Fig. 9. It indicates the simple function of surface roughness and specific grinding energy. According to the inversely linear relation proposed by Malkin, the above theoretical derivation is believable. It is believed that the grinding process changes the material removal mode, resulting in the variation of specific grinding energy, and then influences the surface roughness. In other words, the surface roughness is not influenced by grain kinematic relation. From formula 8, it can be seen that it is difficult to accurately predict the surface roughness of brittle materials only by grinding process parameters. Based on the specific grinding energy, the surface roughness prediction can be made, in which more process and material performance parameter can be omitted. The formula is simple and convenient.

$$\begin{cases} u = \dfrac{P'}{Q'}, \quad Q' = v_w \cdot a_p \\ P' = 6.4 \times 10^{-20} \left(K_c^{3/2} H S_w^{'} \right) \\ S_w^{'} = \left(\dfrac{6C}{\sin 2\theta} \right)^{1/2} \left(v_w v_s \right)^{1/2} a_p^{3/4} d_s^{1/4} \end{cases} \tag{6}$$

Where, u is the specific grinding energy; P is the grinding energy per unit width; Q is the material removal rate per unit width; K_c is the fracture toughness; H is the vicker hardness; S'_w is the ratio of groove area; C is the grain density per unit area ($2.5mm^{-2}$), θ is the grain half vertex angle (θ=60°); v_w is the workpiece speed; v_s is the grinding velocity; a_p is the cutting depth and d_s is the diameter of grinding wheel.

$$u \propto \left(\frac{v_w}{v_s} \right)^{-\frac{1}{2}} \tag{7}$$

Where, u is the grinding energy; v_w is the workpiece speed, and v_s is the grinding velocity.

$$Ra \propto \frac{1}{u} \tag{8}$$

In order to describe the high-speed grinding performance of K9 glass, it is compared with SiC (silicon carbide) under the same high-speed grinding process. The surface roughness under the grinding velocity of 80m/s is shown in Fig 10. The variation range of SiC is *Ra*0.87-1.01μm and that of K9 glass is *Ra*1.18-1.78μm. From Fig 10, it can be seen that under the same grinding and dressing process, SiC has lower surface roughness than K9 glass. Therefore, K9 glass is more difficult to

cut and its surface tends to brittle fracture more easily. The specific energy can be calculated based on formula (4) and (6), which is used to indicate the relation between the surface roughness and specific grinding energy (as shown in Fig 9). From Fig.9, it can be seen that the specific energy of SiC is larger than that of K9 glass. Due to high fracture toughness K_c (3.2MP•$m^{1/2}$) and hardness, it is much higher than that of K9 glass. The greater the surface roughness of K9 glass, the greater the difficulty of cutting.

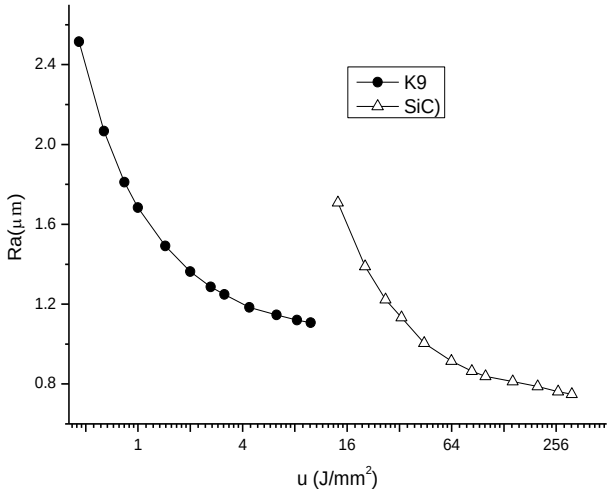

Fig. 9. The relation between the specific grinding energy and surface roughness

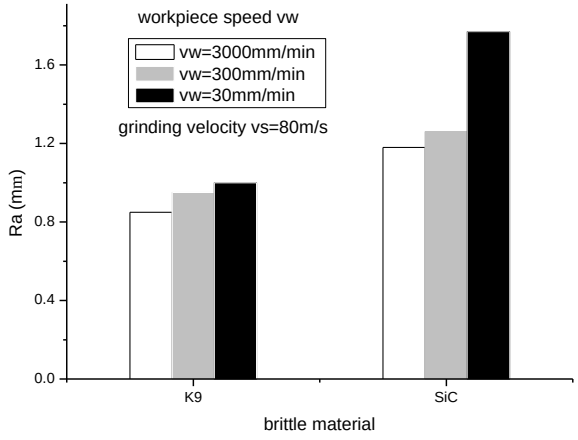

Fig. 10. Surface roughness comparison between K9 glass and SiC

5. Conclusion

High-speed grinding of K9 optical with monolayer brazed diamond grinding wheel is studied in the paper. The variation of ground surface roughness Ra, the roughness ratio Ra/Rz and Ra ratio between normal and parallel grinding direction with grinding velocity variation has been tested. The main conclusions are as follows:

(1) The removal of K9 glass grinding is mainly brittle. Ground surface consists of uneven pits and less parallel marks. In low speed grinding, several 25μm surface defects appear, while there is few larger surface defects in high-speed grinding.

(2) The variation range of ground surface *Ra* of K9 glass is 1.23-1/85μm. Ra decreases with the increase of grinding velocity and the decrease of workpiece. With the increase of grinding speed, the roughness ratio $\frac{Rz}{Ra}$ decreases obviously, this indicates that the larger surface defects decrease with the increase of grinding speed. The roughness ratio of normal and parallel direction increases with the increase of grinding velocity, which indicates that the continuity of grinding texture continuity is improved and the removal mode tend to be ductile.

(3) The previous surface roughness prediction model focuses on grinding process parameters. Since K9 glass has its distinct material performance, material performance must be considered in the prediction model. A concise formula is derived to show the inverse relation between the surface roughness and specific energy, which is helpful to predict the surface roughness.

Acknowledgement

The work is supported by major scientific research program of Henan universities and colleges (20A460011), key scientific research projects of colleges and universities in Henan Provinc(20A460011), and Key R & D and promotion projects in Henan Province(202102210064).

REFERENCES

[1]. *SH. Yin; JM. Cao, S. Gong etc.* Research on process of high-efficiency precise dicing optical glass. Diamond & abrasive engineering. vol. 39, pp. 54-59, 2019. DOI: 10.13394/ j.cnki.jgszz.2019.1.0010. 2019.

[2]. *J. Du; ZJ. Li; H. Gong etc.* Study on mechanism and control method of edge chipping fracture in the machining of brittle and hard material. Mechanical Science and technology for aerospace and engineering. vol. 32, pp. 1451-1455. 2013.

[3]. *HN. Li; TB. Yu; LD. Zhu, etc.* Evaluation of grinding-induced subsurface damage in optical glass BK7. Journal of materials processing technology, vol. 229, pp. 785-794, DOI: 10.1016/j.jmatprotec.2015.11.003. 2016.

[4]. *QL. Zhang; S. To; QL. Zhao, etc.* Surface generation mechanism of WC/Co and RB-SiC/Si composites under high speed grinding. Int. Journal of refractory metals and hard materials, vol. 56, pp. 123-131, DOI: 10.1016/j.ijrmhm.2015.12.002. 2016.

[5]. *J. Cheng; GQ. Yinl Q. Wen.* Study on grinding force modelling and ductile regime propelling technology in micro drill-grinding of hard and brittle materials. Journal of materials processing technology. vol. 223, pp. 150-163, 2015. DOI: 10.1016/j.jmatprotec.2015.04.005. 2015

[6]. *B. Zhang; YC. Fu.* Grinding of brittle materials with brazed diamond grinding wheel. International journal of advanced manufacture technology. vol. 67, pp. 2845-2852, 2013. DOI: 10.1007/s00170-012-4697-8. 2013

[7]. *ST. Chen; ZH. Jiang.* A force controlled grinding-milling technique for quartz-glass micromachining. Journal of materials processing technology. vol. 216, pp. 206-215, 2015 DOI: 10.1016/ j.jmatprotec.2014.09.017. 2015.

[8]. *B. Guo; Q. Zhao; X. Fang.* Precision grinding of optical glass with laser micro-structured coarse-grained diamond wheels. Journal of materials processing technology, vol. 214, pp. 1045-1051, DOI: 10.1016/j.jmatprotec.2013.12.013. 2014.

[9] *QL. Zhao; B. Guo.* Ultra-precision grinding of optical-glasses using mono-layer nickel electroplated coarse- grained diamond wheels, Part 2:investigation of profile and surface grinding. Precision grinding, vol. 39, pp. 67-78, 2015. DOI: 10.1016/j.precisioneng.2014.07.007

[10] *K. Zhang; J.Sun; H.Wang etc.* (2016): Experimental research on high speed grinding of silicon nitride ceramic spindle. CONFERENCE: Materials Science Forum, vol. 874, pp. 253-258, DOI: 10.4028/www.scientific.net/MSF.874.253,

[11] *Kaiomchaiyakul. J.* Abrasive machining of ceramics: assessment of near-surface characteristics in high speed grinding. State of Connecticut: University of Connecticut. 2000

[12] *Arif. M; Zhang.XQ; Rahman.M.* A predictive model of the critical undeformed chip thickness for ductile–brittle transition in nano-machining of brittle materials. International Journal of Machine Tools & Manufacture. vol. 64, pp. 114-122, 2013. DOI: 10.1016/j.ijmachtools. 2012.08.005

[13] *DH. Zhu; SJ. Yan; BZ.Li.* Single-grit modeling and simulation of crack initiation and propagation in SiC grinding using maximum undeformed chip thickness. Computational material science, vol. 92, pp. 13-21, 2014. DOI: 10.1016/j.commatsci.2014.05.019

[14] *Malkin. S; Cai.GQ, Kong. YD;* Grinding technology theory and its application. MONOGRAPH: Shenyang: Northeast university press. pp. 137-158, 2002

[15] *YZ. Zhang.* Metal cutting principle. Beijing: Aeronautic industry press. pp. 407-409, 1988

[16] *TW. Hwang.* Grinding energy and mechanisms for ceramics. Massachusetts: State university, 1996